CONF-890387--2

Anomalous Positrons from Heavy Ion Collisions

- Past Results and Future Plans

CONF-890387--2

DE89 009800

R. R. Betts

Physics Division

Argonne National Laboratory

Argonne, Illinois 60439

DISCLAIMER

This report was prepared as an account of work sponsored by an agency of the United States Government. Neither the United States Government nor any agency thereof, nor any of their employees, makes any warranty, express or implied, or assumes any legal liability or responsibility for the accuracy, completeness, or usefulness of any information, apparatus, product, or process disclosed, or represents that its use would not infringe privately owned rights. Reference herein to any specific commercial product, process, or service by trade name, trademark, manufacturer, or otherwise does not necessarily constitute or imply its endorsement, recommendation, or favoring by the United States Government or any agency thereof. The views and opinions of authors expressed herein do not necessarily state or reflect those of the United States Government or any agency thereof.

Abstract

The current status of the experimental study of anomalous lines observed in the spectra of positrons produced in heavy ion collisions is reviewed. A new experiment to measure positron-electron coincidences is discussed.

MASTER

Invited talk presented at the "Workshop on Highly Charged Ions: New Physics and Advanced Techniques" Lawrence Berkeley Laboratory March 13-15, 1989.

DISTRIBUTION OF THIS DOCUMENT IS UNLIMITED

The submitted manuscript has been authored by a contractor of the U. S. Government under contract No. W-31-109-ENG-38. Accordingly, the U. S. Government retains a nonexclusive, royalty-free license to publish or reproduce the published form of this contribution, or allow others to do so, for

1. INTRODUCTION

The availability of high intensity beams of the heaviest ions has made possible the search for new effects which can occur as a result of the extremely high electric fields produced in collisions of these ions with heavy atoms [1]. An area of work which has produced one of the most tantalizing results in physics today, is the study of positron emission in these collisions. The initial motivation for this work was the search for the spontaneous emission of positrons which is expected to occur for systems whose combined charge exceeds that for which the K-shell binding energy exceeds $2m_ec^2$. In such cases, a vacancy in the K-shell produced early in the collision will appear as a spontaneously produced positron as the vacancy dives into the negative energy continuum. This process has not yet been identified, primarily due to the relatively weak signal as compared to a continuous background of positrons produced by the rapidly varying fields which occur in the ion-ion collision. Instead, an unexpected feature has been observed [2-5] in the spectra of positrons - a sharp line, the explanation of which as so far eluded us. The possibility that the positron line phenomenon represents some new physics makes its understanding one of the important questions of the day. In this talk I will review the status of the current experiments and some possible explanations and describe the plans for future experiments in this area.

2. EXPERIMENTAL APPARATUS

Three distinct experimental programs have been pursued, all at the Gesellschaft für Schwerionenforschung (GSI) Darmstadt. The three collaborations are: "EPOS" - Frankfurt, GSI, Heidelberg, Mainz, Yale; "ORANGE" - GSI, Munich and "TORI" - Darmstadt, GSI. The EPOS spectrometer [6], in its most recent configuration, is shown schematically in Fig. 1. It consists of a solenoid mounted transverse to the beam direction. Heavy ions are detected in parallel

plate avalanche counters mounted above and below the horizontal plane. On one side of the solenoid, a spiral baffle selects trajectories corresponding to positrons which are subsequently detected on-axis with a cylindrical, cooled Si(Li) detector. Positrons are identified by the coincident detection of their characteristic annihilation radiation in an annular, segmented NaI detector which surrounds the Si(Li) detector. On the other side, coincident electrons are detected in two planar Si(Li) detectors mounted parallel to and displaced from the solenoid axis, facing so as to select electron trajectories. Further details of this apparatus are given in Ref. 6.

The ORANGE apparatus [7-8], again in its most recent form, is shown in Fig. 2. Two toroidal spectrometers of the focussing orange type are placed facing each other along the beam direction. Heavy ions are detected in an array of parallel plate avalanche counters which cover the entire range of azimuthal angles. The field in the backward orange is set to focus positrons which are detected in a cylindrical array of 60, cooled silicon detectors arranged about the beam axis in the form of a "pagoda". The identification of positrons is accomplished by the requirement that the momentum derived from the focal plane position (detector segmentation) corresponds to the measured kinetic energy from the silicon. This requirement enables the rejection of essentially all background processes as well as backscattering from the silicon. The forward orange is set to focus and detect electrons.

The third apparatus [9], "TORI", consists of two quarter toroids as shown in Fig. 3. Positrons and electrons are separated by the different sense of the drift motion in the non-uniform field. Electrons are detected in detectors placed either on the middle-plane diaphragm (0°) where they are spatially separated from the positrons, or in a detector placed on the opposite side of the beam direction (180°). Positrons are detected after passage through the second half of the torus in which the drift direction is reversed. The positrons are identified by their annihilation radiation.

3. EXPERIMENTAL RESULTS

The observation of sharp peaks in the energy spectrum of positrons measured in coincidence with sub-Coulomb barrier, heavy-ion scattering is the major reason for the intense current interest in this field [2-5]. Examples of these data are shown in Figs. 4 and 5. The narrow peaks appear superimposed on a broad, continuous background which is well accounted for by the results of calculations [10] based on quasi-atomic processes plus a contribution from internal pair producing nuclear transitions deduced from the measured gamma ray spectrum. The strength of the lines can be enhanced relative to the continuous background by selection of certain ranges of heavy-ion scattering parameters, the line appearing more prominently for larger scattering angles. The exact details of the dependence of the positron line production on the specifics of the heavy ion scattering remain to be explored. In particular, no consistent picture of the energy dependence of the positron production cross-section has emerged. The cross-section for the line structure appears to be more or less independent of heavy ion scattering angle [11] as shown in Fig. 6.

The peak phenomenon has been investigated in a wide range of heavy ion systems ranging from Th+Ta (Z_u=163) to U+Cm (Z_u=188). The differing resolutions of the various experiments and the limited statistics of the data make firm conclusions difficult but the following statements can be made [12]; the energies of the observed lines are independent of Z_u, the lines appear in systems both above and below the value of Z_u for which spontaneous positron emission is expected [Z_{cr}=173] and all high resolution data show more than one line in each collision system. These results are summarized in Fig. 7.

The dependence of the line cross-section on Z_u is shown in Fig. 8. The data are fit [12] with a $Z_u^{22\pm2}$ dependence which is similar to the Z_u^{20} dependence expected for the dynamically produced continuum positrons and provides the connection between the line production mechanism and the intense electromagnetic fields which occur during the collision.

The narrow widths of the observed lines is one of the most surprising features of the experimental observations. The measured widths of the lines correspond to times 10^{-19} to 10^{-20} s, considerably longer than the average collision times which, for Coulomb trajectories, are 10^{-21} s. Taking into account the large angular range accepted by the apparatus, the data are all consistent [5] with the observed line resulting from monoenergetic emission of positrons in a frame moving with the center-of-mass velocity of the heavy ion system. As shown in Fig. 9, the transverse velocity of the source is constrained to be small, such that emission from one of the reseparated scattered nuclei is excluded.

The independence of the line energies on Z_u suggests an origin common to all the collision systems. The narrow peak widths further raise the possibility of a two-body decay which could result from the electron-positron decay of some previously unknown, neutral object. This scenario has prompted a number of coincidence experiments in which the energy correlation of the positron lines with coincident electrons has been investigated.

For the two-body decay of an object (x) into e^+-e^- pairs, the total energies of the positron and electron in the laboratory frame are given by

$$E_{e+}^{LAB} = \gamma\ (E_{e+}^{cm} + \beta\ P_{e+}^{cm}\ \cos\theta_{e+}^{cm})$$

$$E_{e-}^{LAB} = \gamma\ (E_{e-}^{cm} + \beta\ P_{e-}^{cm}\ \cos\theta_{e-}^{cm})$$

where β,γ refer to the velocity with which x was produced. Therefore

$$E_{e+}^{LAB} + E_{e-}^{LAB} = \gamma\ (E_{e+}^{cm} + E_{e-}^{cm}) = \gamma\ M_x c^2$$

because

$$\theta_{e+}^{cm} = (\pi - \theta_{e-}^{cm}) \quad \text{and} \quad P_{e+}^{cm} = P_{e-}^{cm}$$

The signature of this process is then, a sharp peak in the sum of the laboratory energies of the positron and electron with a width smaller than the singles

positron or electron peak width, providing the spread in velocities with which x is produced is not too large. Further, the difference energy spectrum should show a peak centered at zero with a width $4\,\beta\,\gamma\,p^{cm}$.

The first results [13] of an experiment of this type for the U+Th at 5.83 MeV/u using the EPOS solenoid are shown in Figs. 10 and 11. For near equal energy electrons and positrons (cut C), a peak appears in the sum energy spectrum as shown in Fig. 11c. This peak is narrower than the peak in the positron spectrum alone and has a width comparable to that expected on the basis of detector resolutions. In this case, the difference energy spectrum for events with the peak sum energy, shown in Fig. 11d, displays a broad peak centered near zero energy difference. This result is consistent with the two-body decay of an isolated object. More recent results [14] with improved detector resolution, reveal sum-energy peaks which are much narrower than the positron singles peaks. In some of these cases, however, the energy differences appear to be no longer centered around zero, although the statistics of the data are rather limited.

To prove the two-body decay hypothesis, information on the angles of emission of the positron and electron is required. The invariant mass of a decaying object

$$M_x c^2 = \gamma^{-1}\,(E_{e+}^{LAB} + E_{e-}^{LAB})$$

$$= \sqrt{2m_e^2c^4 + 2\left(E_{e+}^{LAB}\,E_{e-}^{LAB} - P_{e+}P_{e-}c^2\cos\theta_{e+e-}\right)}$$

depends on the energies of the positron and electron and also their opening angle. For small source velocities, as are suggested by the positron singles measurements, the opening angle in the laboratory frame is close to 180°. The EPOS spectrometer, although not allowing the direct determination of the angles, does have an acceptance which allows a broad selection of opening angles. In

some cases, the data are consistent with back-to-back decay. In others, however, there is a preference for non back-to-back decays [14].

Some more direct information comes from a recent measurement [15] by the ORANGE group. The acceptance of the double orange, together with the segmentation of the silicon detector arrays, allows the selection of data into one of four opening angle bins. The data are consistent with near back-to-back emission although unfortunately the statistics are rather limited.

4. THEORETICAL IDEAS

Many of the features of the data are consistent with the two-body decay of a slowly moving neutral object. The apparent independence of the line energies on the details of the heavy ion scattering system suggests the formation of an elementary object. From the multiplicity of lines it would appear necessary to postulate either a family of elementary particles with masses 1.5-1.8 MeV or an object possessing internal structure. At first, before the several different peaks had been seen, it appeared that a variant of the long-sought axion could possibly account for the experimental observations. This possibility was later ruled out in a series of direct experimental searches [16]. More recently, it has been suggested that a new form of positronium - bound at short distances - might exist and thus be a candidate [17]. Such a possibility is not ruled out by our current understanding of quantum electrodynamics [18]. A more exotic explanation is based on the results of lattice gauge calculations which suggest [19] that a transition to a confining phase of quantum electrodynamics might occur in the strong fields produced in the heavy ion collisions. In this case [20], the new phase possesses a set of bound states analogous to positronium in the normal phase of quantum electrodynamics. A schematic calculation of such a mass spectrum produces a number of meson-like states which decay to positron electron pairs by tunneling to the normal weak coupling phase.

All these suggestions require production of particle like object decaying to positron-electron pairs.

Numerous other explanations which do not produce two-body like decays have been proposed. These range from the production of long-lived di-nuclear states [21] which then enhance and give monoenergetic spontaneous production, to interference effects [22] and, most recently [23], collective excitations of the electron gas surrounding the ions which then decay by pair emission.

5. FUTURE EXPERIMENTS

The most pressing and important experimental question is a resolution of the two-body decay hypothesis. Any new experiment should therefore allow the determination of the angles of emission of the positrons and electrons and thus the invariant mass of the object producing the pair. In addition, it is clear that the apparently slow progress in the field has resulted largely from the difficulty in obtaining data. A new experiment should therefore have a much higher data collection efficiency than the current experiments.

A major difficulty with low energy positrons and electrons is the multiple scattering they undergo in passing through material. This precludes the use of angle measurement by multiple measurement of the trajectory as is conventionally done at higher energies. The necessity to transport the positrons away from the target to a region where the detector can be shielded from the intense backgrounds produced in the heavy-ion collisions, requires the use of schemes where a single position measurement can be related to the angle of emission.

A proposal for a new experiment to do this has recently been submitted [24]. The experiment consists of a new large solid angle spectrometer to be placed at the Argonne superconducting linac accelerator ATLAS. The experiment has been given the acronym ATLAS Positron Experiment - APEX. A schematic drawing of the proposed APEX spectrometer is shown in Fig. 12. It consists of a

large, weak field (300 Gauss) uniform field solenoid, mounted transverse to the beam direction. The field is produced by 18 pancake coils equally spaced over a distance of 2.1 m. Positrons and electrons spiral down the solenoid, undergoing several turns before being detected in a thin pencil-shaped array of silicon detectors. Each of these arrays consists of 216, 3 cm x 0.5 cm, 1 mm thick PIN diodes arranged on the surface of a hexagonal cylinder 36 cm long with 1.5 cm sides. Positrons are identified by their characteristic annihilation photons, both of which are detected in a cylindrical array of NaI crystals. These crystals are specially made with rather short attenuation lengths such that the pulse height information from both ends of a crystal can be used to determine the position of the annihilation photons [25] and thus reconstruct the position on the silicon array where the annihilation took place. Both the silicon arrays and the annihilation radiation detectors are shielded from a direct view of the target by two conical heavy-metal plugs placed on either side of the target. These plugs have the additional function of intercepting the trajectories of the intense flux of low-energy δ-rays which would otherwise swamp the silicon detectors. The main physical properties of APEX are listed in Table I.

The angular acceptance of this device is shown as a function of energy in Fig. 13 and the total acceptance is displayed in Fig. 14. A comparison of this device with the GSI EPOS and ORANGE spectrometers is given in Table II. The total acceptance of the APEX spectrometer for back-to-back coincidences is approximately a factor of four larger than for EPOS or ORANGE.

The angle information is obtained from a combination of energy, position and time-of-flight of the detected particles. The angle with respect to the solenoid axis is given by

$$\theta = \mathrm{acos}\left(\frac{p_z}{p}\right)$$

where p_z, the component of momentum along the solenoid axis, is determined from the time-of-flight and the detection position. The total momentum p is calculated from the measured energy. An important feature of this device is that the spiral orbits always have close to a complete number of turns and the time-of-flight is then an integer times the cyclotron period.

$$T = \frac{2\pi E_{TOT}}{eB\ c^2}$$

Thus, providing the time-of-flight resolution is sufficient to determine how many turns a given particle has undergone ($\Delta t \lesssim 2$ns), the total time-of-flight can be determined to the precision of the kinetic energy measurement. The requirement that the time resolution of the electron and positron detectors be less than the spiral period is the governing factor in the determination of the field strength and thus the scale of the apparatus. Measurements with prototype PIN diodes [26], cooled to liquid nitrogen temperature, lead us to expect a time resolution of better than 2 ns and an energy resolution of 5 keV. The ϕ measurement is determined by the azimuthal segmentation of the silicon array which in the current design corresponds to $\pm 10°$.

A detailed Monte Carlo simulation of the apparatus indicates that the angular resolution of the device will be limited by multiple scattering in the target (300 μgm/cm^2), provided the expected time resolution of better than 2 ns is obtained. This, in turn, corresponds to a determination of the invariant mass of a hypothetical particle with a resolution of approximately 25 keV FWHM.

In addition to the increased acceptance of the new apparatus, the ATLAS accelerator also provides important advantages over the GSI UNILAC. The duty factor of ATLAS is 100%, compared to the 25% of the UNILAC. To the extent that the current GSI experiments are limited by high instantaneous counting rates, for the same instantaneous current, ATLAS therefore gives a factor of four advantage, provided the targets are able to withstand the increased time

averaged beam intensity. The total improvement in count rate is therefore over an order of magnitude. For near equal energy, back-to-back positron electron pairs produced with the cross-section for the lines measured at GSI and a 10 pnA beam incident on a 300 $\mu gm/cm^2$ target, the event rate is calculated to be 0.3 s^{-1}. This should allow high statistics data to obtained in a relatively short period of time.

The construction time scale of APEX is linked to the upgrade of ATLAS which is currently under way. The first phase of this upgrade - replacement of the tandem injector with an ECR positive ion source and new injector linac - is now complete. The final phase, production of uranium beams, is expected to be finished at the end of 1990. The APEX experiment is therefore planned to start taking data in early 1991.

This research was supported by the U.S. Department of Energy, Nuclear Physics Division, under contract W-31-109-ENG-38.

Table I. Properties of the APEX Solenoid

Vacuum Vessel:	
Length:	4 m
Diameter:	1 m
Field:	
Number of Coils:	18
Field in Central Region:	300 Gauss
Silicon Detector Arrays (2):	
Position of Front of Array:	120 cm from target
Length of Array:	36 cm
Radius of Array:	1.5 cm
Active Area:	270 cm^2
Number of Detector Elements:	216 per array
Detector Thickness:	1 mm
Annihilation Radiation Detectors (2):	
Number of Crystals:	24 per detector
Number of Phototubes:	48 per detector
Length of Detector:	50 cm
Inner/Outer Diameter of Detector:	40/52 cm
Heavy-Ion Counter:	
Number of Segments:	36
Angle Coverage:	20 - 70°
Average Flight Path:	45 cm
Gas:	Isobutane
Gas Pressure:	5 Torr

Table II. Comparison of APEX, EPOS and ORANGE Spectrometers

	APEX	EPOS	ORANGE
Energy Acceptance (keV)	200-650	100-900	250-550[a)]
Singles Positron Efficiency	9.0%	9.6%	3.3%
Positron - Electron Coincidence Efficiency[b)]	5.6%	1.4%	1.5%

[a)] This energy acceptance is obtained by scanning the field of the spectrometer. For a fixed field the energy acceptance is ~100 keV and the positron singles efficiency 10%. The coincidence efficiency is 4.4%.

[b)] For near equal energy back-to-back particles

References

[1] For recent reviews see, Quantum Electrodynamics of Strong Fields, ed. W. Greiner, (Plenum, New York, 1983) and Physics of Strong Fields, ed. W. Greiner, (Plenum, New York, 1987).

[2] J. Schweppe et al. Phys. Rev. Lett. 51 (1983) 2261.

[3] M. Clemente et al. Phys. Lett. 137B (1984) 41.

[4] H. Tsertos et al. Phys. Lett. 162B (1985) 273.

[5] T. Cowan et al. Phys. Rev. Lett. 54 (1985) 1761.

[6] T. Cowan, Ph.D. Thesis, Yale University (1988) (unpublished).

[7] P. Kienle, Physica Scripta T23 (1988) 123.

[8] E. Berdermann et al. Nucl. Phys. A448 (1988) 683c.

[9] M. Krämer et al. in Physics of Strong Fields, ed. W. Greiner (Plenum, New York 1987) p. 441.

[10] U. Müller et al. Z. Phys. A313 (1983) 263.

[11] H. Tsertos et al. Z. Phys. A328 (1987) 499.

[12] W. Koenig et al. Z. Phys. A328 (1987) 129.

[13] T. Cowan et al. Phys. Rev. Lett. 56 (1986) 444.

[14] H. Bokemeyer in Proceedings of XXIV International Conference on High Energy Physics, August 1988 Munich, ed R. Kotthaus and J. H. Kühn (Springer-Verlag, Berlin 1989) p. 1441.

[15] W. Koenig et al. Phys. Lett. 218B (1989) 12.

[16] R. D. Peccei et al. Phys. Lett. 172B (1986) 435.

[17] C. Y. Wong in Windsurfing the Fermi Sea, ed. T. T. S. Kuo and J. Speth (Elsevier, Amsterdam, 1987) vol. 2, p. 296.

[18] B. Müller in Atomic Physics of Highly Ionized Atoms, ed. R. Marrus (Plenum, New York, in press).

[19] R. D. Peccei et al. Phys. Rev. D37 (1988) 2492.

[20] D. G. Caldi and A. Chodos, Phys. Rev. D36 (1987) 2876.

[21] J. Rafelski et al. Z. Phys. A285 (1978) 49.

[22] T. de Reus et al. J. Phys. G12 (1986) L303.

[23] J. M. Bang et al. Z. Phys. A330 (1988) 431.

[24] The APEX Collaboration; Argonne, Florida State, Michigan State, Princeton and Yale.

[25] A. J. Court et al. Nucl. Instr. and Meth. A273 (1988) 706.

[26] Supplied by MICRON Semiconductor, Lancing, England.

Figure Captions

Fig. 1. Schematic drawing of the EPOS spectrometer.

Fig. 2. The ORANGE spectrometer.

Fig. 3. Schematic view of the TORI spectrometer.

Fig. 4. Positron energy spectra for six collision systems measured by the EPOS group. The peaks are enhanced relative to the background by cuts on the heavy ion scattering parameters.

Fig. 5. Positron energy spectra for U+U and U+Th measured by the ORANGE group. The range of heavy ion scattering angles is indicated on the figure. The curves show the calculated continuum due to quasi-atomic and nuclear processes (N).

Fig. 6. Differential cross-section for line production versus heavy-ion scattering angle for U+U and U+Th.

Fig. 7. Energies of positron lines observed in the high resolution work of Ref. [12] plotted versus Z_u (solid points). Energies from the low resolution measurement in Ref. [3] are shown as open circles.

Fig. 8. Dependence of the line cross-section on Z_u. The solid line shows a Z_u^{22} dependence.

Fig. 9. The measured width of the positron peak as a function of heavy ion scattering angle. The width is expressed as the ratio of the measured width to that expected for emission from the center-of-mass frame. The curves show the dependence expected for emission from different sources.

Fig. 10. Intensity distribution of coincidence events as a function of positron and electron energy for 5.83 MeV U+Th measured by the EPOS group. Also shown are the projections onto the positron and electron energy axes. The cuts labelled A-D are used in generating the spectra a-d in Fig. 11.

Fig. 11. Spectra generated using the cuts A-D shown in Fig. 10. These spectra shown; a) a peak in the positron spectrum, b) a corresponding peak in the electron spectrum, c) a peak in the sum-energy spectrum and d) a peak in the difference energy spectrum.

Fig. 12. Schematic illustration of the APEX apparatus. Major components are labelled. For the sake of clarity, the heavy ion detectors have been omitted - they will cover the angular range from 20°-70° with respect to the beam direction and have complete azimuthal coverage. The silicon detector arrays are placed at 1.2 m from the target position and the inner diameter of the annihilation radiation detectors is 40 cm.

Fig. 13. APEX angular acceptance shown as a function of energy (shaded area). Theta is the angle with respect to the solenoid axis. The acceptance is symmetric with respect to rotations about this axis.

Fig. 14. Total detection efficiency for positrons in the APEX spectrometer. This includes all geometric effects, the silicon detector efficiencies and the annihilation radiation detection efficiency. Above 650 keV, the efficiency falls rapidly due to transmission of the positrons through the 1 mm thick silicon detectors.

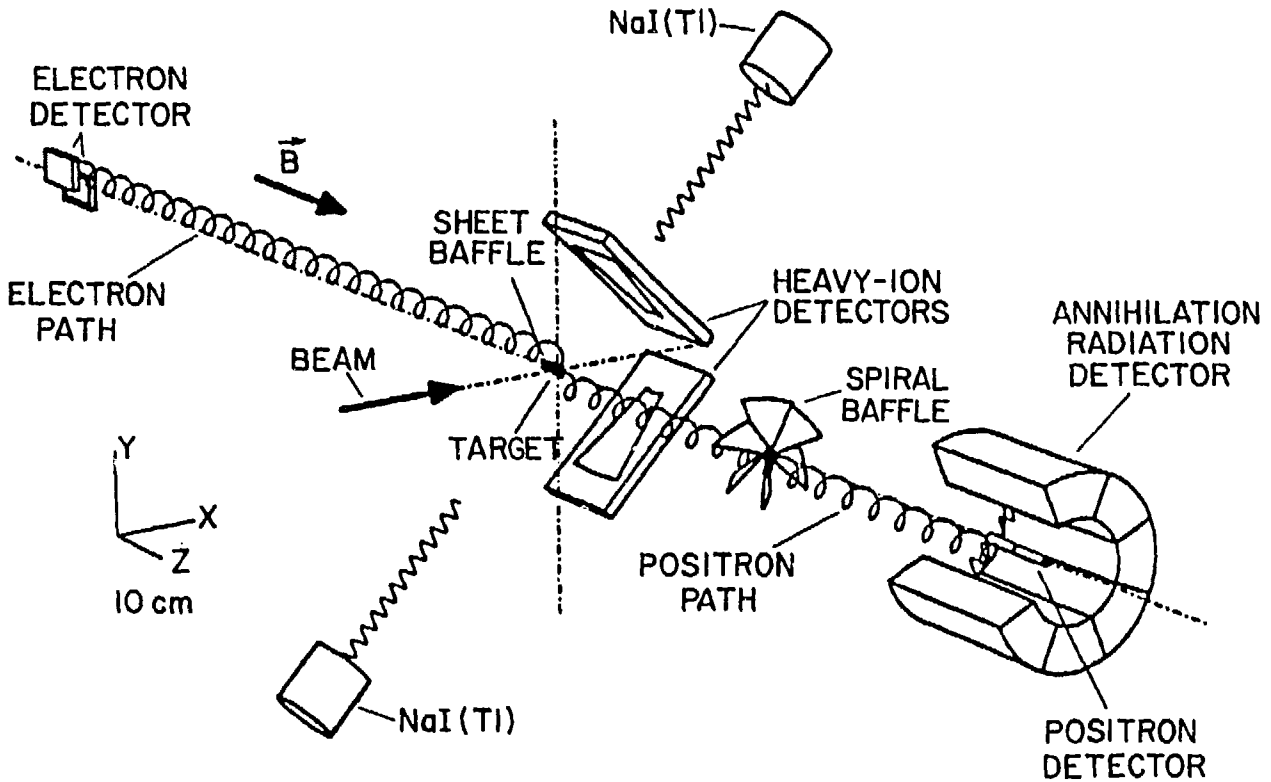
NaI(Tl)
ELECTRON DETECTOR
B
SHEET BAFFLE
HEAVY-ION DETECTORS
ANNIHILATION RADIATION DETECTOR
ELECTRON PATH
BEAM
SPIRAL BAFFLE
TARGET
Y
X
Z
10 cm
POSITRON PATH
NaI(Tl)
POSITRON DETECTOR

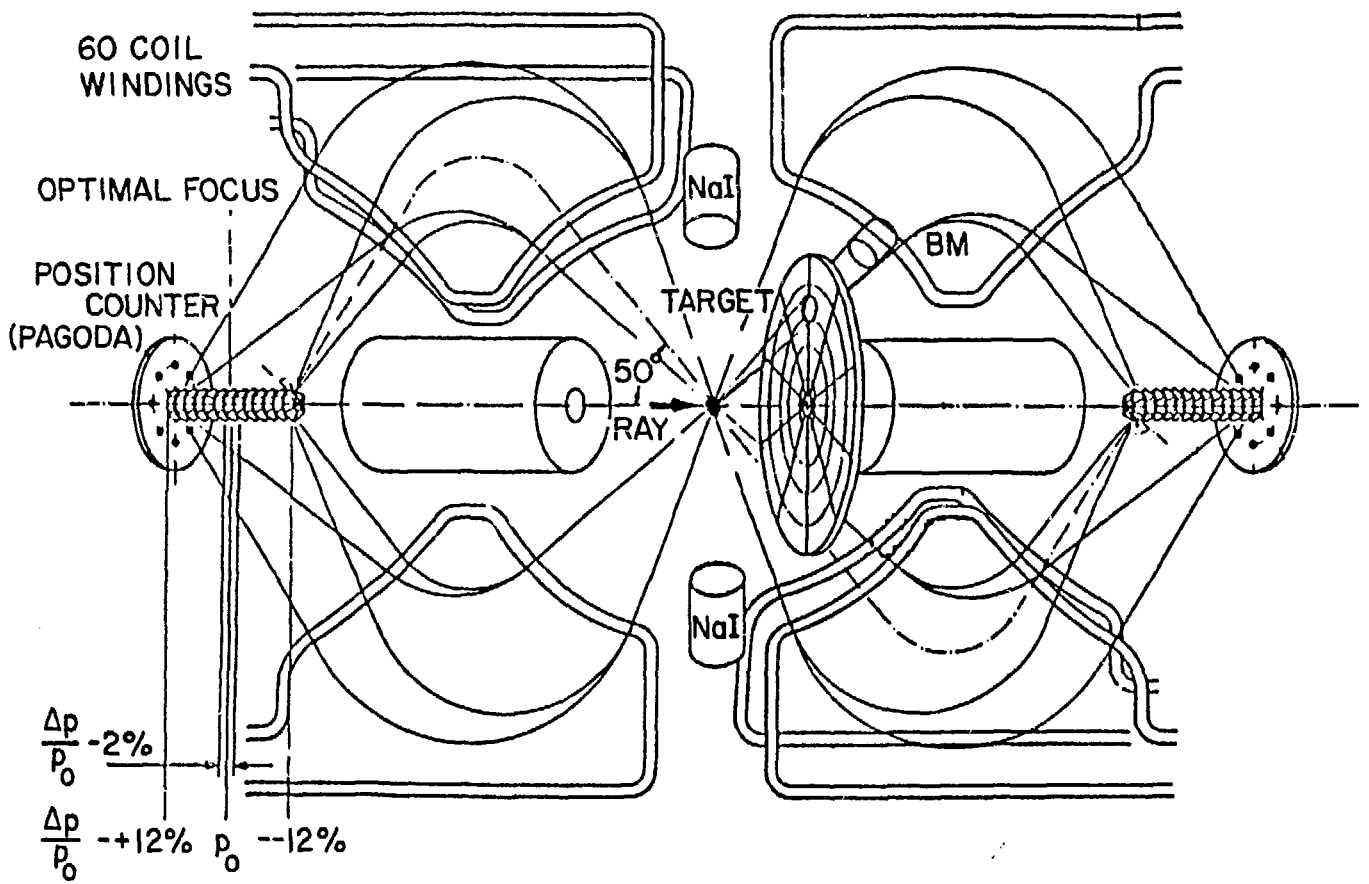
60 COIL
WINDINGS
OPTIMAL FOCUS
POSITION
COUNTER
(PAGODA)
NaI
BM
TARGET
50°
RAY
NaI
Δp/p0 -2%
Δp/p0 -+12%
p0
--12%

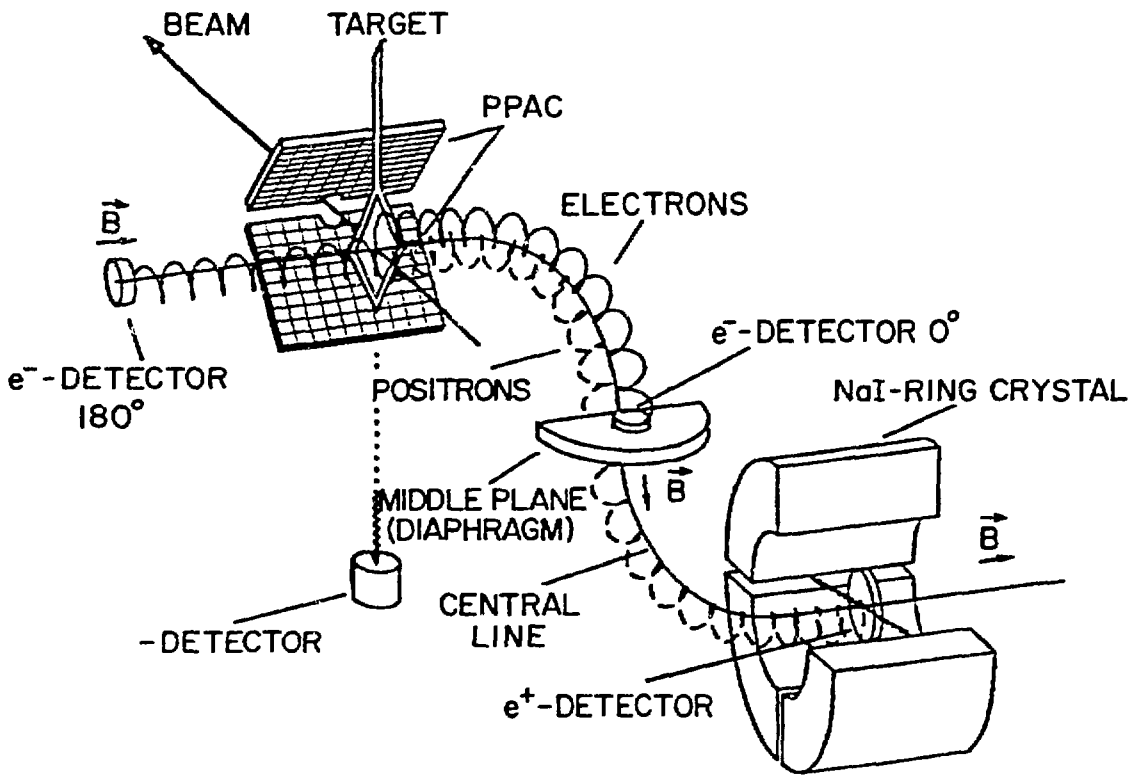
BEAM
TARGET
PPAC
ELECTRONS
B
e⁻-DETECTOR 0°
e⁻-DETECTOR
180°
POSITRONS
NaI-RING CRYSTAL
MIDDLE PLANE
(DIAPHRAGM)
B
B
CENTRAL
LINE
-DETECTOR
e⁺-DETECTOR

Fig

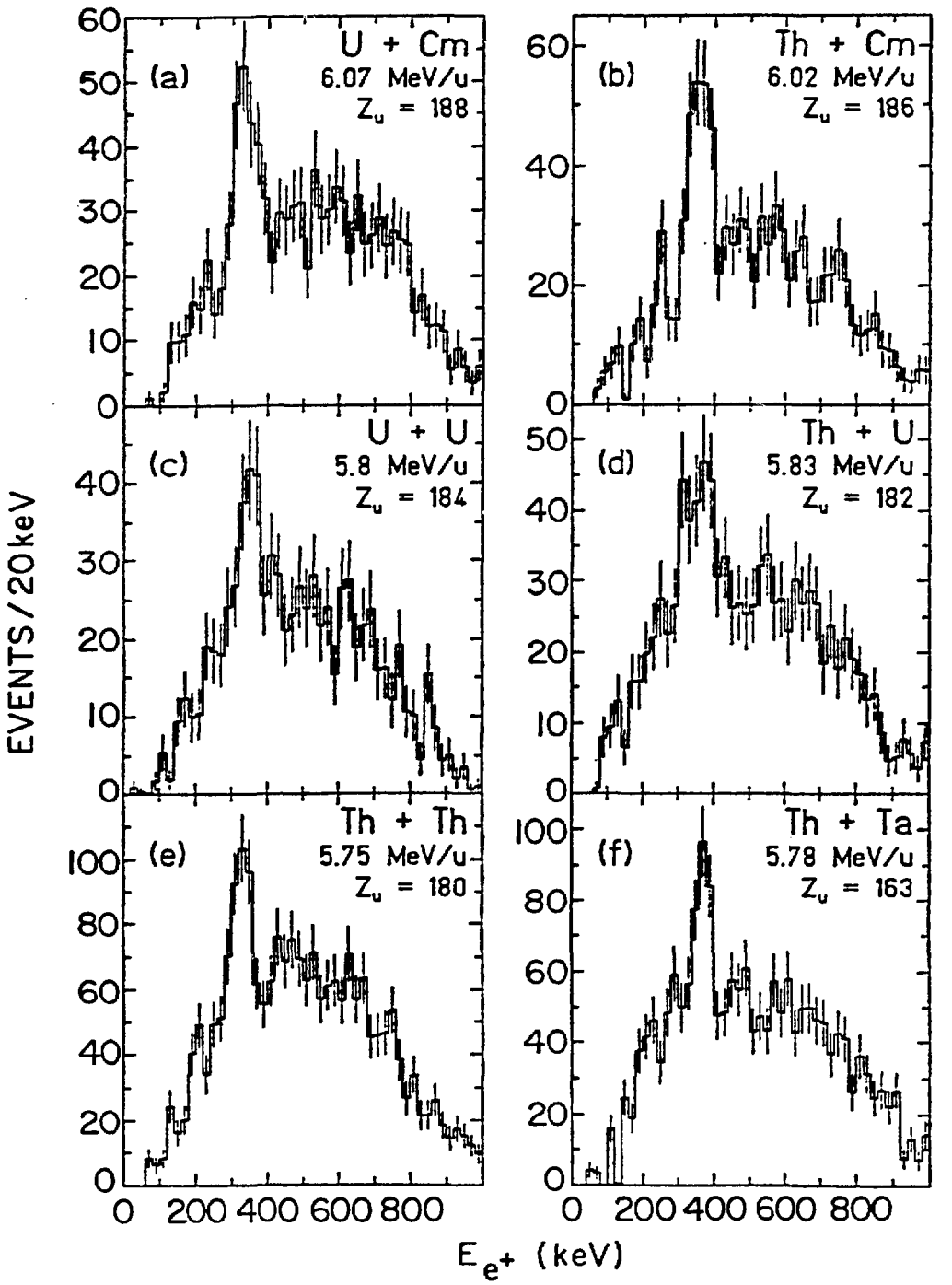
(a)
U + Cm
6.07 MeV/u
Z_u = 188
(b)
Th + Cm
6.02 MeV/u
Z_u = 186
(c)
U + U
5.8 MeV/u
Z_u = 184
(d)
Th + U
5.83 MeV/u
Z_u = 182
(e)
Th + Th
5.75 MeV/u
Z_u = 180
(f)
Th + Ta
5.78 MeV/u
Z_u = 163
EVENTS/20keV
E_{e^+} (keV)

Fig 4

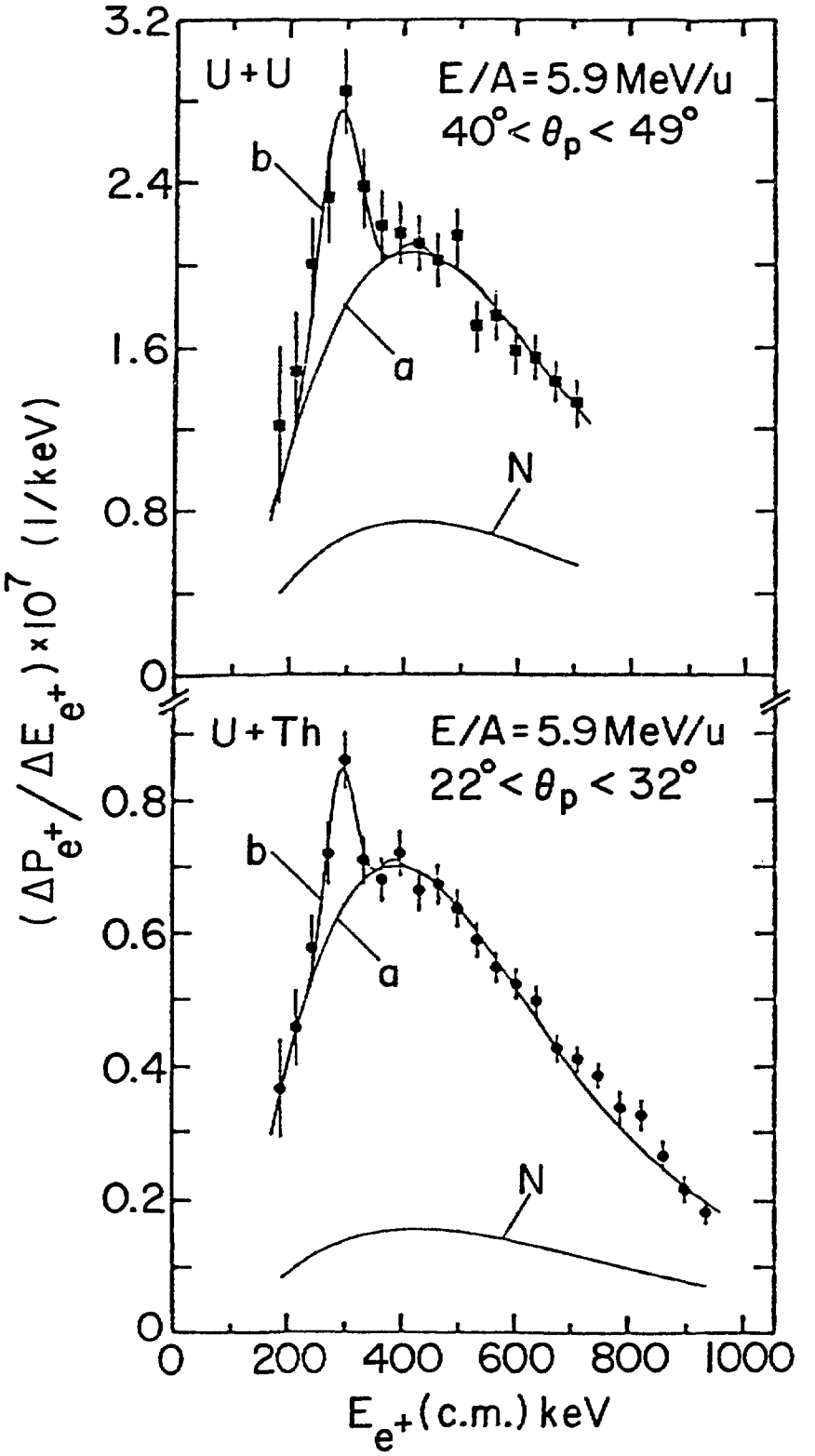
U+U
E/A=5.9 MeV/u
40°< θp < 49°
b
a
N
U+Th
E/A=5.9 MeV/u
22°< θp < 32°
b
a
N
3.2
2.4
1.6
0.8
0
0.8
0.6
0.4
0.2
0
0
200
400
600
800
1000
(ΔPe+/ΔEe+)×10^7 (1/keV)
Ee+(c.m.) keV

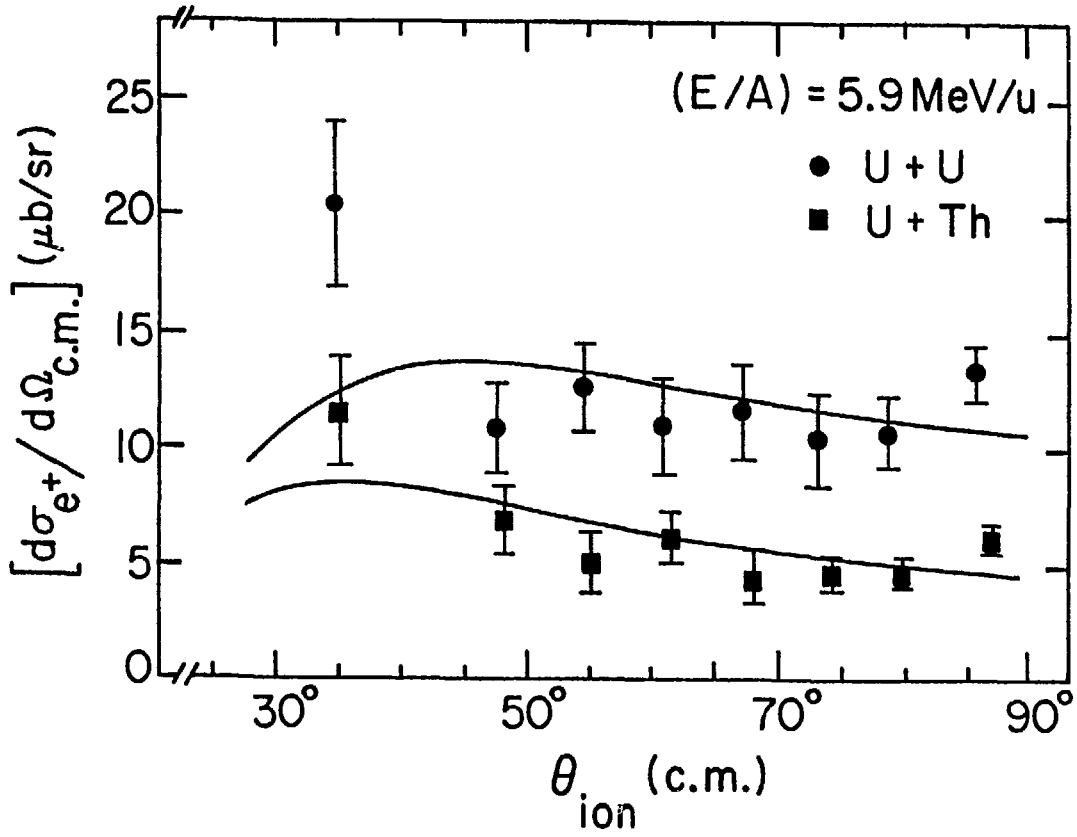
(E/A) = 5.9 MeV/u
U + U
U + Th
25
20
15
10
5
0
30°
50°
70°
90°
θ_{ion} (c.m.)
$[d\sigma_{e^+}/d\Omega_{c.m.}]$ (μb/sr)

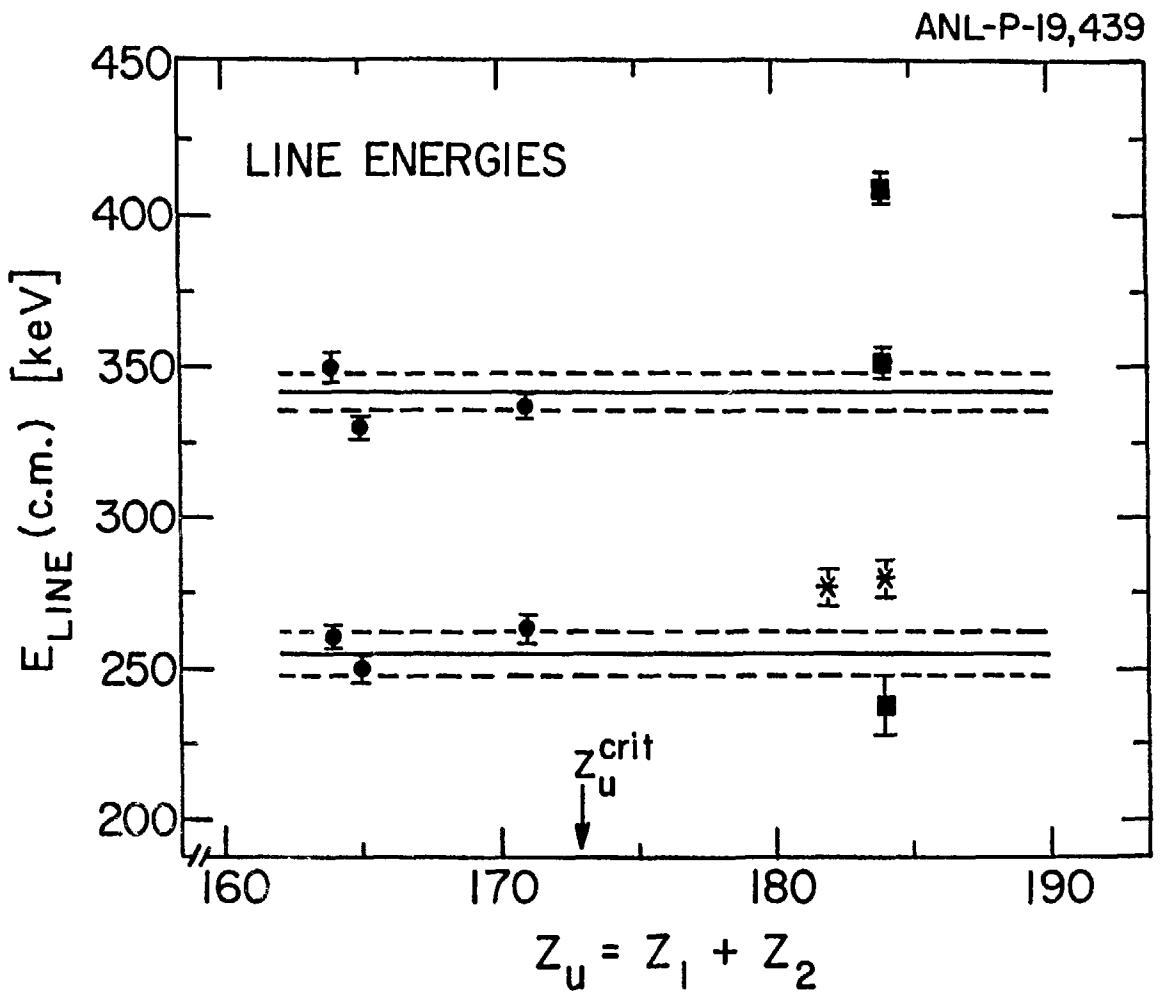
ANL-P-19,439
LINE ENERGIES
450
400
350
300
250
200
E_{LINE} (c.m.) [keV]
Z_u^{crit}
160
170
180
190
$Z_u = Z_1 + Z_2$

ANL-P-19,440

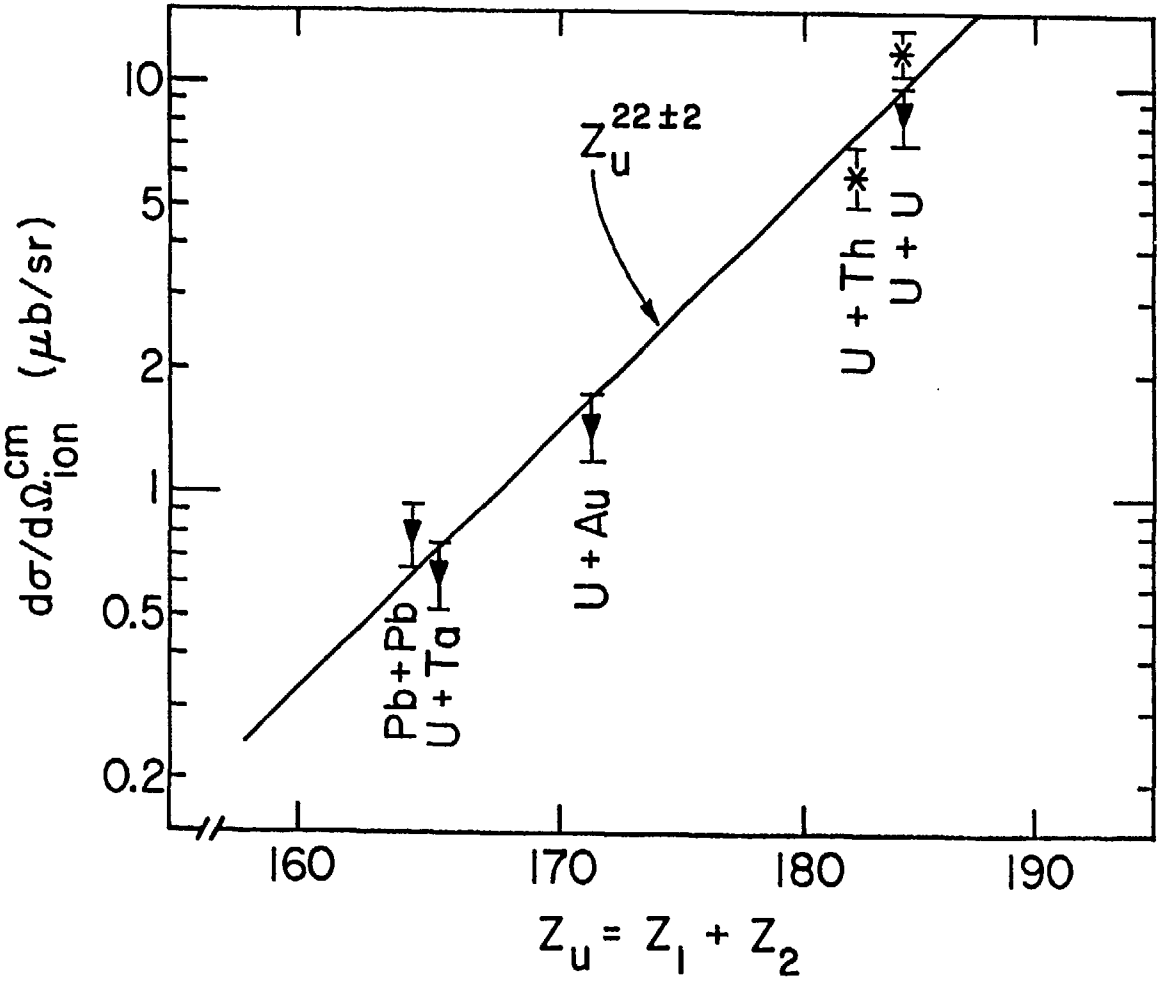
$d\sigma/d\Omega^{cm}_{ion}$ (μb/sr)
10
5
2
1
0.5
0.2
$Z_u^{22\pm2}$
Pb+Pb
U+Ta
U+Au
U+Th
U+U
160
170
180
190
$Z_u = Z_1 + Z_2$

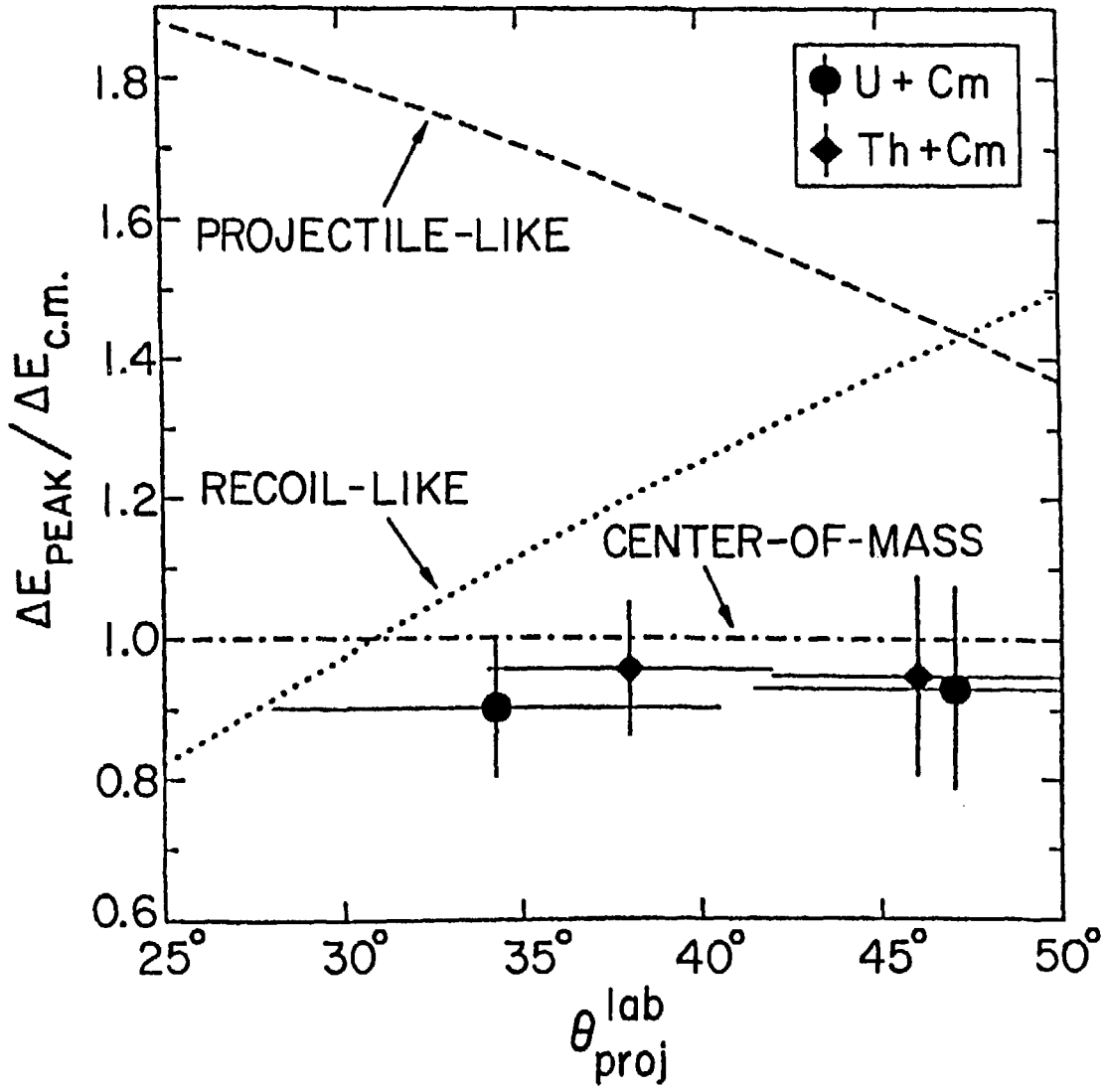
U + Cm
Th + Cm
PROJECTILE-LIKE
RECOIL-LIKE
CENTER-OF-MASS
1.8
1.6
1.4
1.2
1.0
0.8
0.6
25°
30°
35°
40°
45°
50°
$\Delta E_{PEAK} / \Delta E_{c.m.}$
θ_{proj}^{lab}

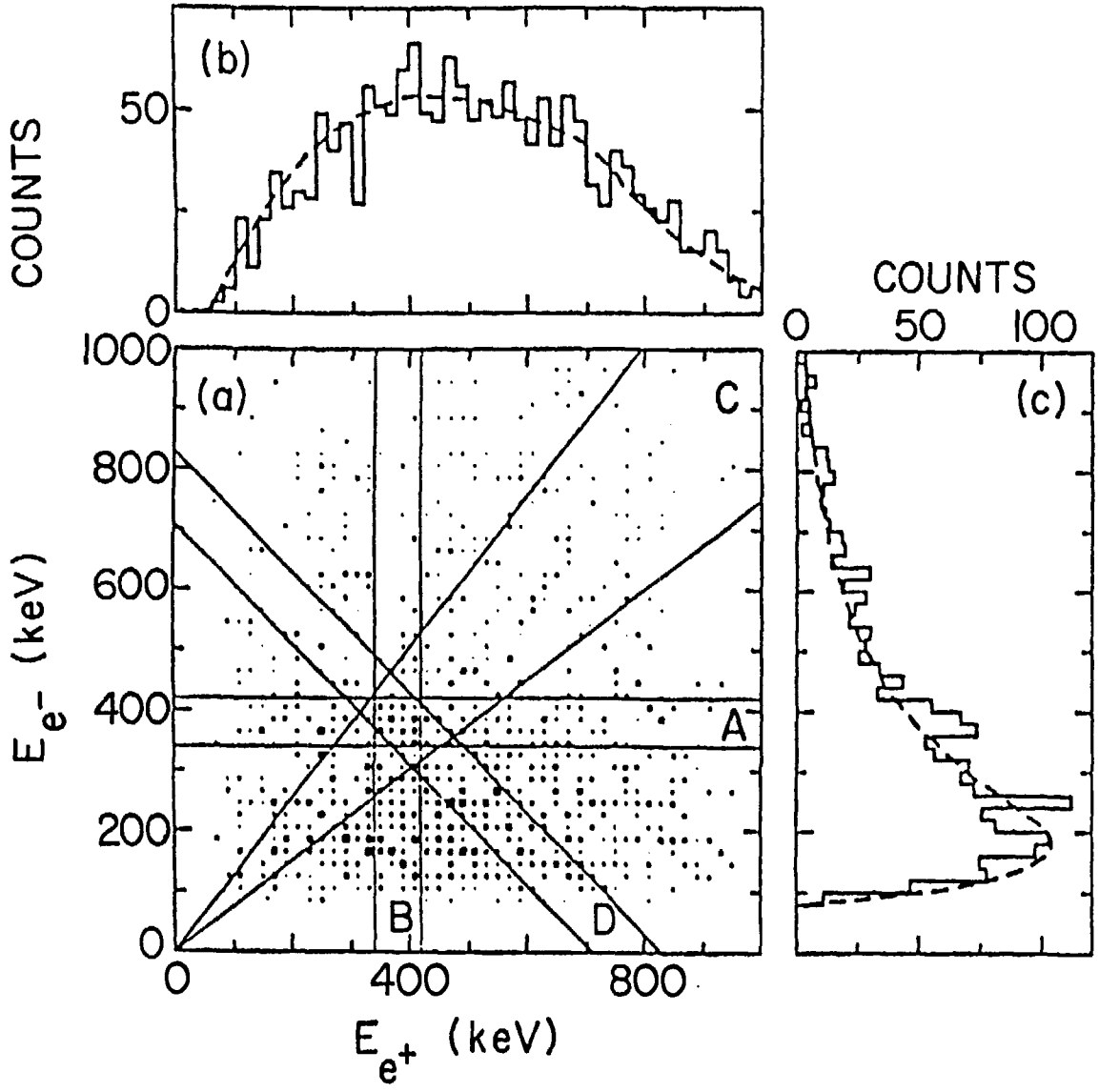
(b)
COUNTS
50
0
(a)
C
A
B
D
1000
800
600
400
200
0
E_{e^-} (keV)
0
400
800
E_{e^+} (keV)
COUNTS
0
50
100
(c)

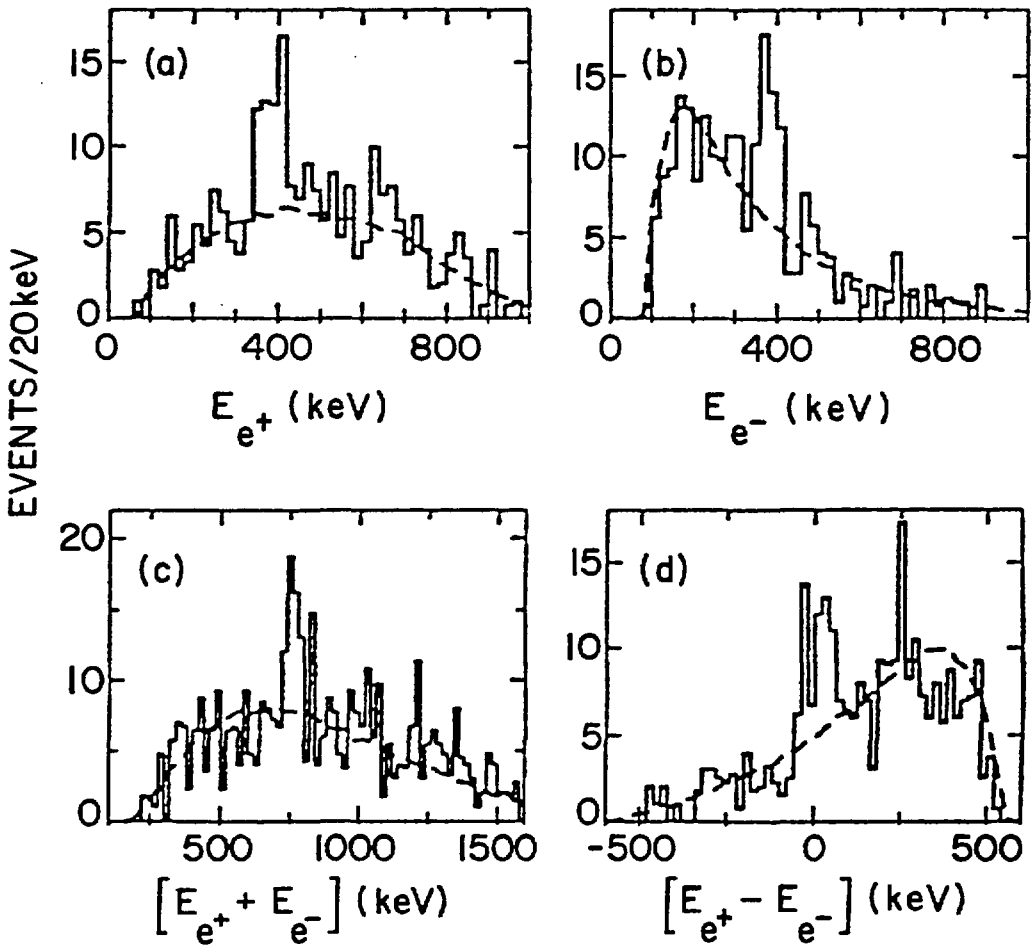
EVENTS/20keV
(a)
(b)
(c)
(d)
E_{e^+} (keV)
E_{e^-} (keV)
$[E_{e^+} + E_{e^-}]$ (keV)
$[E_{e^+} - E_{e^-}]$ (keV)

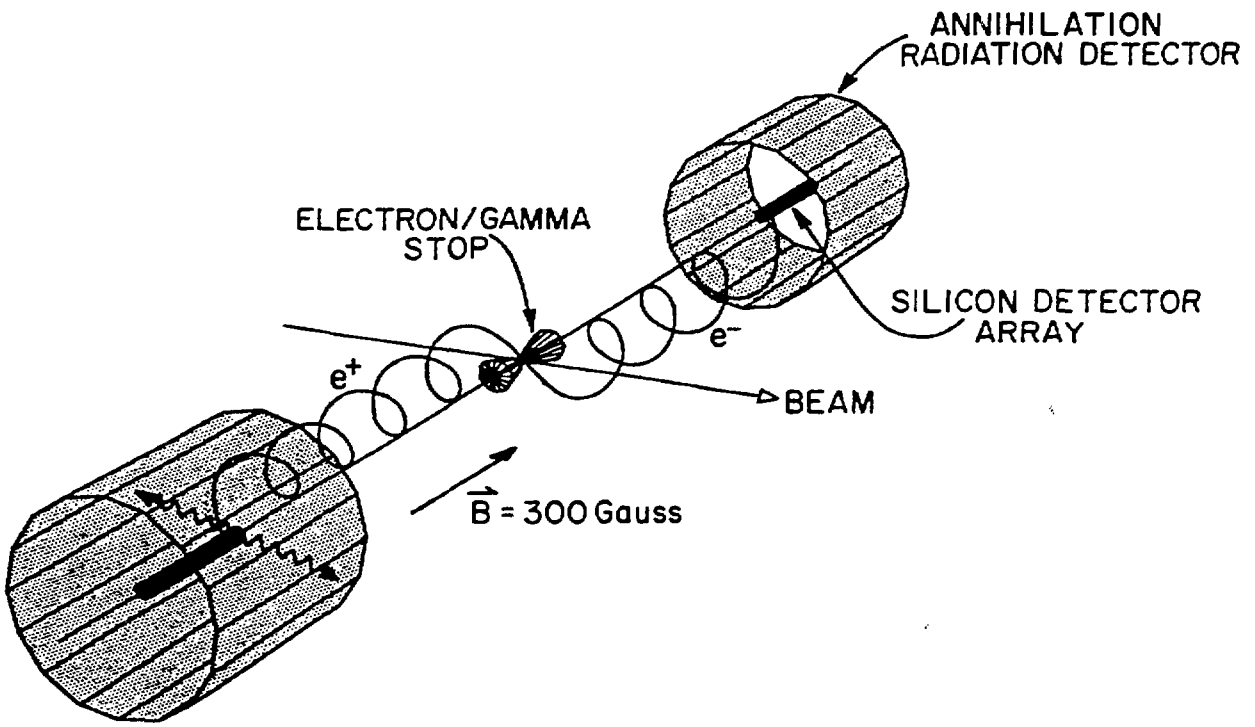
ANNIHILATION
RADIATION DETECTOR
ELECTRON/GAMMA
STOP
SILICON DETECTOR
ARRAY
e⁻
e⁺
BEAM
B = 300 Gauss

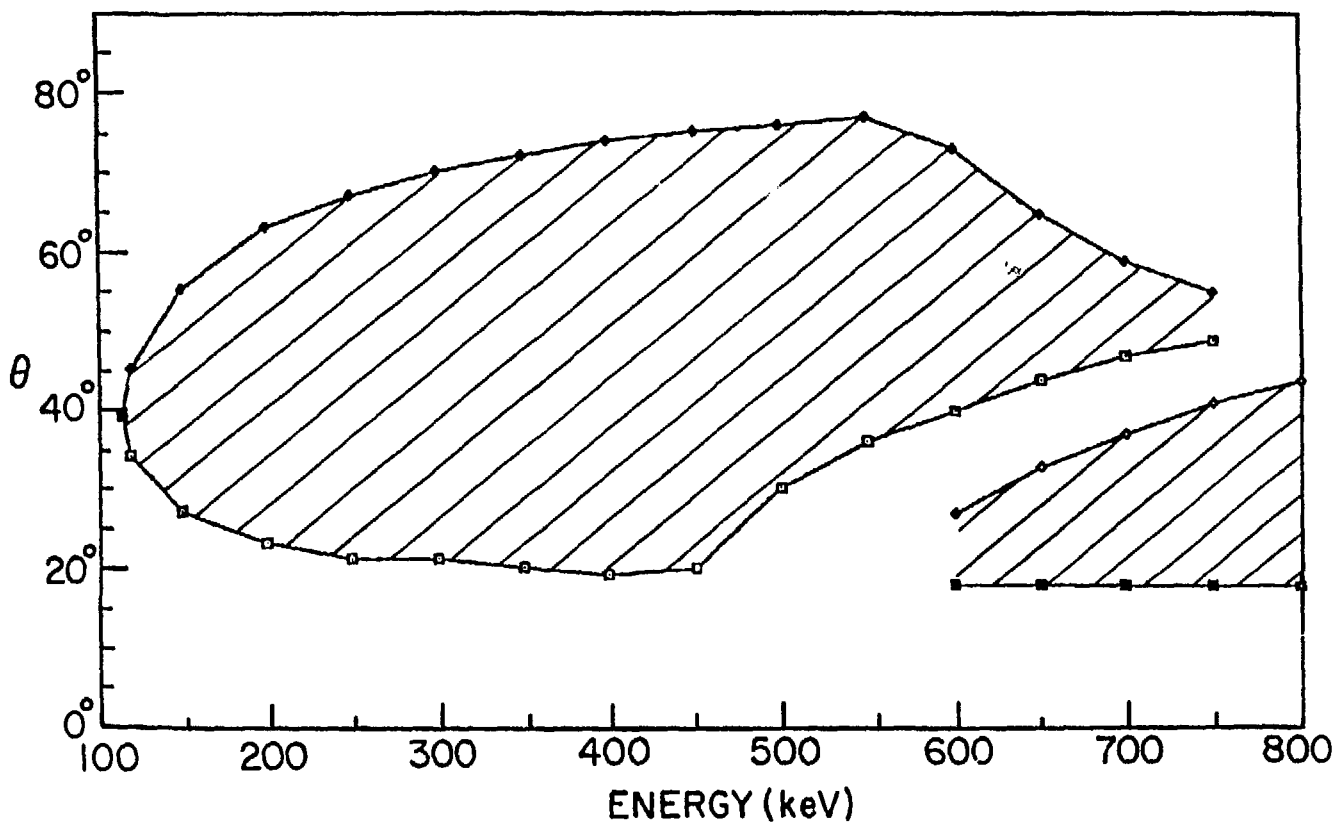
80°
60°
θ
40°
20°
0°
100
200
300
400
500
600
700
800
ENERGY (keV)

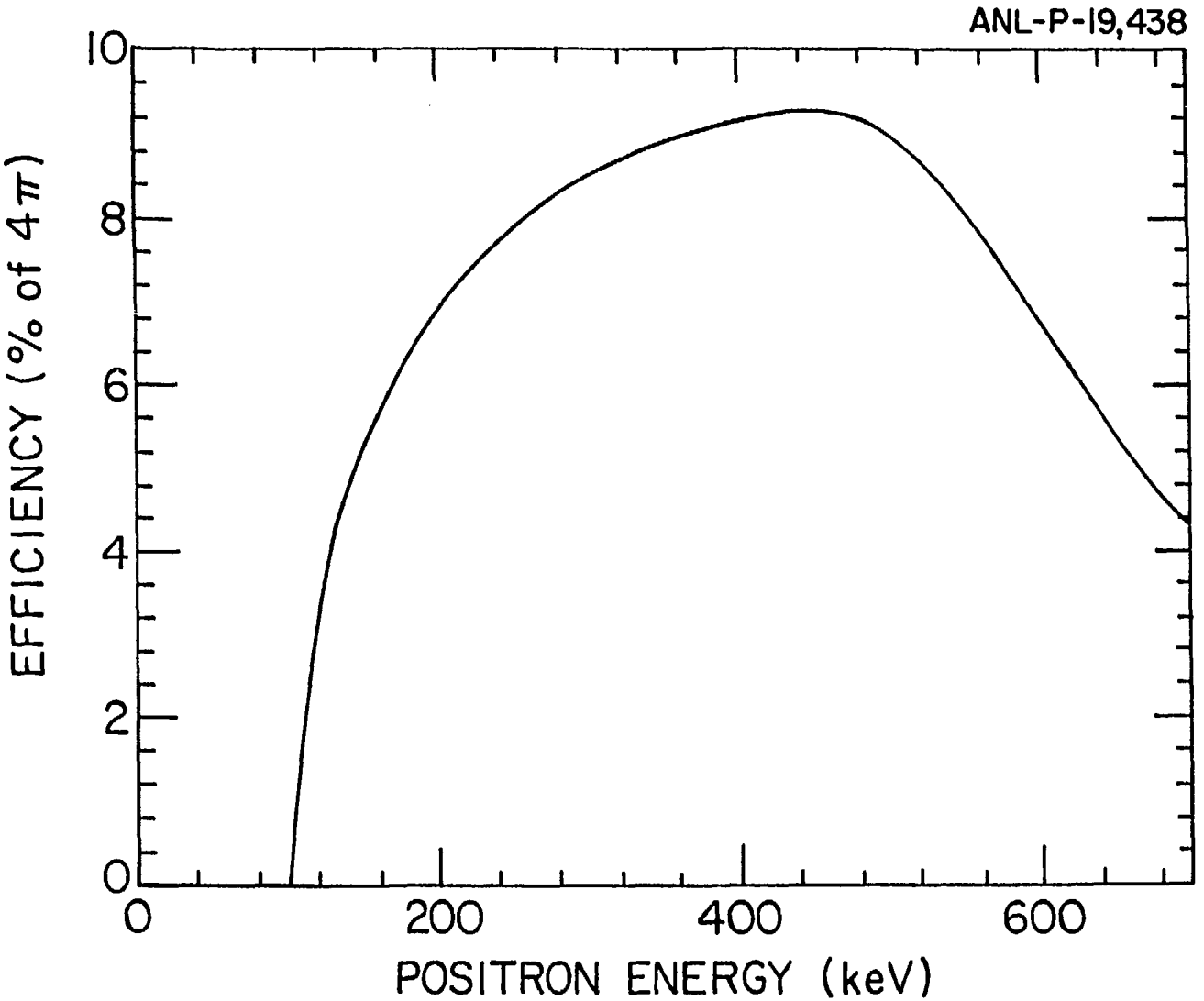
ANL-P-19,438
EFFICIENCY (% of 4π)
10
8
6
4
2
0
0
200
400
600
POSITRON ENERGY (keV)